

000 001 002 003 004 005 006 007 008 009 010 011 012 013 014 015 016 017 018 019 020 021 022 023 024 025 026 027 028 029 030 031 032 033 034 035 036 037 038 039 040 041 042 043 044 045 046 047 048 049 050 051 052 053 OPTIMIZING TEMPORAL AND SPATIAL EFFICIENCY FOR CHAIN-OF-THOUGHT REASONING IN LARGE LANGUAGE MODELS

Anonymous authors

Paper under double-blind review

ABSTRACT

Chain-of-Thought (CoT) reasoning in Large Language Models (LLMs) achieves remarkable performance but suffers from significant computational overhead. CoT reasoning exhibits redundancy across two critical dimensions: temporal redundancy, where reasoning steps may be unnecessary, and spatial redundancy, where computations can be performed at reduced precision. While existing approaches require expensive dataset construction and model fine-tuning to improve reasoning efficiency, we propose *Temporal-Spatial Adaptive Reasoning (TSAR)*, a training-free framework that jointly exploits both redundancy dimensions through coordinated optimization. TSAR segments reasoning based on Dewey’s reflective thinking model, employs progressive precision reduction that adapts to both reasoning phases and progress, and coordinates termination decisions through entropy-based confidence estimation. Our adaptive scheduler prevents precision-induced errors while enabling compound efficiency gains. Extensive evaluation on diverse reasoning tasks demonstrates up to $12.4 \times$ speedup while maintaining the accuracy, establishing coordinated multi-dimensional redundancy exploitation as superior to conventional optimization strategies.

1 INTRODUCTION

Chain-of-Thought (CoT) reasoning has revolutionized how Large Language Models (LLMs) approach complex problem-solving, enabling systematic decomposition of intricate tasks through step-by-step reasoning (Wei et al., 2022; Parashar et al., 2025). However, this approach often produces long reasoning chains that are computationally expensive, as they require generating and processing a greater number of tokens across multiple intermediate steps, leading to higher inference latency, memory consumption, and energy demands (Sui et al., 2025; Feng et al., 2025). This poses significant challenges for practical deployment, particularly in resource-constrained environments.

Existing approaches to improve CoT reasoning efficiency predominantly rely on training-dependent methods that require substantial computational resources and domain-specific data collection. Training-based methods construct specialized datasets and fine-tune models to reduce reasoning steps (Liu et al., 2024; Xia et al., 2025), but suffer from limited transferability across domains. Structural optimization approaches modify reasoning strategies through prompt engineering (Kang et al., 2024), but often sacrifice reasoning completeness for efficiency and require extensive manual optimization. Computational optimization techniques apply general LLM efficiency methods like uniform quantization (Zhang et al., 2025) or simple confidence-based early exit (Qiao et al., 2025) to reasoning tasks, but treat reasoning as generic text generation, missing reasoning-specific optimization opportunities and failing to exploit the multi-dimensional nature of redundancy in CoT reasoning.

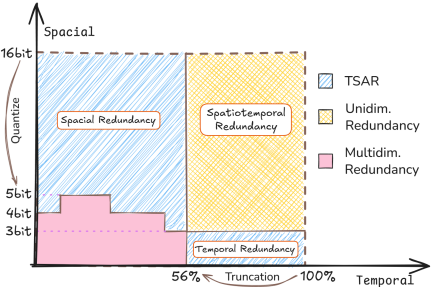


Figure 1: Reducing temporal and spatial redundancy is critical to optimize the efficiency of reasoning LLMs.

The fundamental challenge in reducing redundancy for CoT reasoning lies in the multi-dimensional nature of inefficiency patterns. Specifically, modern reasoning LLMs exhibit redundancy across two critical dimensions (Figure 1): **temporal redundancy** where entire reasoning steps become unnecessary once sufficient understanding is achieved (Sui et al., 2025; Li et al., 2024), and **spatial redundancy**, where individual computations can be performed at reduced precision without significant quality degradation (Zhang et al., 2025). These redundancy dimensions are inherently correlated—they emerge from the same underlying reasoning dynamics and exhibit strong dependencies that current approaches systematically ignore. To effectively reduce these redundancies to optimize the inference efficiency of reasoning LLMs, there are several critical challenges that need to be addressed.

Challenge 1: Redundancy Detection and Exploitation. Identifying when reasoning steps become redundant requires a sophisticated understanding of reasoning progress and confidence dynamics. Simple heuristics like fixed confidence thresholds fail to capture the complex patterns of reasoning completion, while training-based approaches require expensive data collection and model modification. The challenge lies in developing training-free methods that can accurately detect redundancy patterns across both temporal and spatial dimensions without compromising reasoning quality.

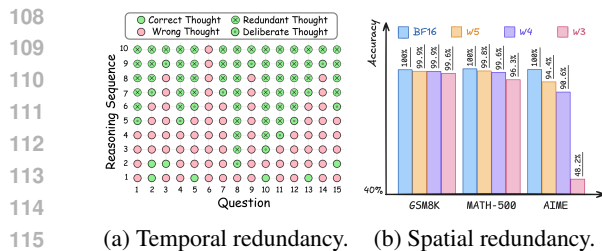
Challenge 2: Multi-Dimensional Coordination. Temporal and spatial redundancy exhibit strong correlations that current independent optimization approaches fail to exploit. When precision reduction affects confidence estimation, termination mechanisms make suboptimal stopping decisions, leading to cascading errors. The challenge is developing coordinated optimization strategies that can exploit these correlations to achieve compound efficiency gains while preventing error propagation between dimensions.

Challenge 3: Dynamic Adaptation to Reasoning Patterns. CoT reasoning exhibits distinct computational phases with heterogeneous redundancy characteristics that static optimization cannot capture. E.g., problem formulation phases require high precision for accurate context establishment, while verification phases often tolerate aggressive quantization and early termination. The challenge lies in developing adaptive strategies that can dynamically adjust policies based on reasoning phase characteristics and temporal progress without requiring training or manual tuning.

To address these challenges, we propose *Temporal-Spatial Adaptive Reasoning (TSAR)*, a training-free framework that jointly optimizes temporal and spatial redundancy through coordinated multi-dimensional exploitation. TSAR operates by automatically segmenting reasoning sequences into distinct cognitive phases based on Dewey’s reflective thinking model, enabling phase-specific optimization policies that adapt to heterogeneous computational requirements. The framework employs progressive precision reduction that dynamically adjusts quantization levels based on both reasoning phase characteristics and temporal progress within the reasoning sequence, moving beyond static uniform quantization to exploit the temporal dependencies inherent in step-by-step reasoning. TSAR coordinates termination decisions through entropy-based confidence estimation computed from thought transition patterns, preventing precision-induced confidence degradation from causing premature or delayed stopping.

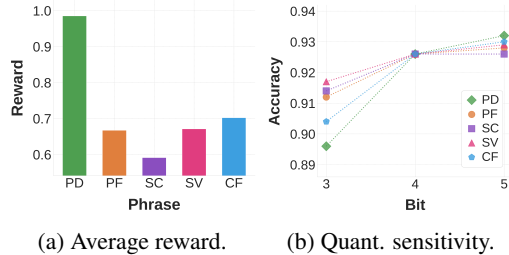
The main contributions of this work can be summarized as follows,

- To the best of our knowledge, TSAR is the first training-free framework that jointly optimizes temporal and spatial redundancy through coordinated, phase-aware scheduling.
- We introduce dynamic precision allocation that adapts to both reasoning phase characteristics and temporal progress, extending beyond static uniform quantization to exploit reasoning-specific computational patterns.
- We establish unified scheduling where precision adaptation informs termination decisions, preventing cascading errors and enabling compound efficiency gains that exceed independent optimization approaches.
- Extensive evaluation on multiple reasoning tasks demonstrates that TSAR achieves up to $12.4\times$ speedup compared to the existing approach, establishing coordinated multi-dimensional redundancy exploitation as substantially superior to conventional efficiency optimization strategies.



(a) Temporal redundancy. (b) Spatial redundancy.

Figure 2: Temporal and spatial redundancy in reasoning LLMs.



(a) Average reward. (b) Quant. sensitivity.

Figure 3: Phase-aware reward and quantization sensitivity in reasoning LLMs.

2 MOTIVATIONS AND OBSERVATIONS

2.1 MULTI-DIMENSIONAL REDUNDANCY ANALYSIS

In order to quantitatively study the redundancy in large reasoning models, we conducted a study on the MATH-500 dataset (Hendrycks et al., 2021b). Our empirical analysis reveals redundancy patterns across two distinct dimensions that exhibit strong correlations, suggesting substantial potential for unified optimization strategies.

Temporal redundancy manifests when reasoning steps become unnecessary once sufficient understanding is achieved. For example, in the verification phases, reasoning often continues beyond the point where confidence stabilizes, with redundant verification steps providing minimal additional value while consuming substantial computational resources. Our analysis in Figure 2 (a) shows that 26.7% of reasoning steps could be eliminated without affecting final answer quality.

Spatial redundancy appears when computations can be performed at reduced precision without affecting reasoning quality. E.g., routine mathematical operations often do not require full precision, while complex analysis demands higher accuracy for numerical stability. Our statistical analysis in Figure 2 (b) reveals that this redundancy is substantial. For a majority of tasks, dramatically reducing precision from full BF16 down to 4-bits (w4), and in some cases even 3-bits (w3), incurs only a negligible drop in accuracy.

2.2 PHASE-BASED COMPUTATIONAL REQUIREMENTS

We hypothesize that CoT reasoning is not a monolithic computational process but rather consists of distinct phases with heterogeneous resource requirements. To test this, we conducted an experiment grounded in the principles of John Dewey’s model of reflective thinking (Dewey, 1933).

Specifically, we split the thoughts generated by LLMs into these phases (with the method introduced in the Methodology Section) and analyze them using a large reward model. Specifically, we employ the reward model Qwen2.5-Math-PRM-7B (Yang et al., 2024) to statistically analyze the scores across these stages, systematically adjusting the precision of each stage to observe its impact on overall accuracy. As illustrated in Figure 3(a), we observe distinct reward magnitudes for different stages. Furthermore, Figure 3(b) reveals their varying sensitivity to quantization. For instance, the Problem Decomposition (PD) phase, which has the highest reward, is highly sensitive to precision, showing a steep decline in accuracy at lower bit-widths. In contrast, other phases like Solution Consolidation (SC) are far more robust to quantization, maintaining high accuracy even at 3-bit precision. This evidence supports our claim that different reasoning phases have distinct computational requirements.

These phase-dependent patterns reveal that optimal efficiency strategies must adapt dynamically rather than apply uniform policies. Static quantization fundamentally cannot capture these variations, leading to systematic resource misallocation where high-redundancy phases receive excessive computational resources while precision-critical phases may be under-provisioned.

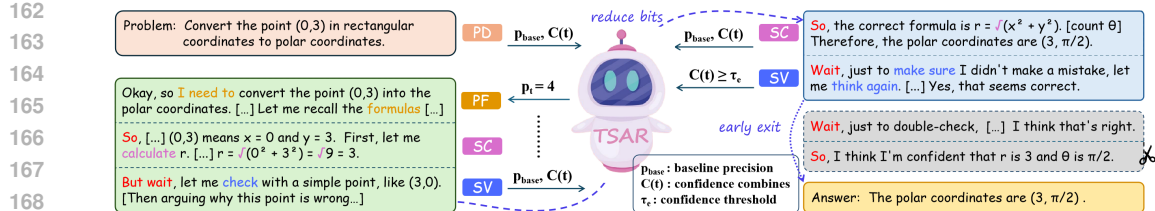


Figure 4: Framework of TSAR, which effectively identifies different reasoning phases, dynamically adjusts their precision levels and timely enables early termination.

3 METHODOLOGY

In this section, we introduce the TSAR framework, depicted in Figure 4, orchestrating phase-aware precision scheduling and entropy-based termination to optimize temporal and spatial efficiency.

3.1 PROBLEM FORMULATION AND REDUNDANCY DEFINITIONS

We formalize the multi-dimensional redundancy optimization problem for CoT reasoning. Consider model M_θ generating reasoning sequence $\mathbf{s} = (s_1, s_2, \dots, s_T)$ given input \mathbf{x} , where the t -th thought s_t is computed using precision $p_t \in \mathcal{P} = \{2, 3, 4, \dots\}$ bits with computational cost $c(p_t)$.

Temporal Redundancy $R_T(t)$ quantifies the unnecessary computational cost from continuing reasoning beyond sufficient understanding:

$$R_T(t) = c(p_t) \cdot \mathbf{1}[t > t^*] \quad \text{where } t^* = \min\{t' \mid \mathcal{Q}(s_{1:t'}) \geq \mathcal{Q}(s_{1:T}) - \epsilon\} \quad (1)$$

where $\mathcal{Q}(\cdot)$ measures reasoning quality and t^* is the optimal reasoning depth and ϵ represents acceptable quality tolerance.

Spatial Redundancy $R_S(t)$ quantifies computational redundancy from precision reduction without quality loss:

$$R_S(t) = c(p_t) - c(p_t^*) \quad \text{where } p_t^* = \min\{p \in \mathcal{P} : \mathcal{Q}(s_t, p) \geq \mathcal{Q}(s_t, p_{max}) - \delta\} \quad (2)$$

where δ represents spatial quality tolerance.

3.2 REASONING PHASE CLASSIFICATION

Inspired by our observation of phase-dependent computational needs, we structure our adaptive framework around a cognitive model. John Dewey’s reflective thinking model, as outlined in his foundational work *How We Think* (Dewey, 1933), provides a cognitive framework for thoughtful inquiry and problem-solving. It describes a sequential process involving five key phases: (1) the recognition of a felt difficulty or problem, (2) the location and intellectualization of the problem (defining it clearly), (3) the suggestion of possible solutions or hypotheses, (4) the development of these suggestions through reasoning and deduction, and (5) the testing of hypotheses through observation, experimentation, or verification, leading to acceptance or rejection.

Building upon this cognitive science foundation, we adapt Dewey’s model to the context of LLM reasoning, distilling it into five distinct phases that align with its core principles while emphasizing heterogeneous computational characteristics. These phases enable targeted optimizations that traditional static approaches cannot exploit effectively:

- Problem Definition (PD), which corresponds to Dewey’s problem recognition (phases 1), focusing on initial context establishment;
- Problem Formulation (PF), which extends the intellectualization by formalizing problem structures, constraints, and representations (phases 2);
- Solution Computation (SC), akin to hypothesis suggestion and initial development (phase 3), involving generative reasoning and derivation;

- Solution Verification (SV), reflecting further reasoning, deduction, and testing (phase 4), emphasizing validation and error checking;
- Conclusion Formation (CF), mirroring final verification and acceptance (phase 5), synthesizing results into a coherent outcome.

We segment reasoning sequences at thought transition points identified by linguistic indicators:

$$\mathcal{S}(s_t) = \mathbf{1}[\exists k \in \mathcal{K}_{split} : k \in s_t] \quad (3)$$

where $\mathcal{K}_{split} = \{\text{"wait"}, \text{"Wait"}, \text{"Alternatively"}, \dots\}$.

In order to ensure operational efficiency, we adopted a keyword-based classification method in the reasoning stage. Specifically, each segment is classified using enhanced phase detection:

$$\Phi(segment) = \arg \max_{\psi \in \Psi} \sum_{k \in \mathcal{K}_\psi} f_k(segment) \quad (4)$$

where $\Psi = \{PD, PF, SC, SV, CF\}$, and f_k is the keyword counting function of keyword k .

3.3 PHASE-AWARE PROGRESSIVE QUANTIZATION

Traditional quantization methods require separate model copies for each precision level, creating prohibitive memory overhead for dynamic switching. Any-Precision maintains a single model that can operate at multiple precisions through nested quantization (Park et al., 2024), enabling seamless precision adaptation essential for reasoning optimization. This capability is particularly valuable for reasoning tasks where precision requirements can change within a single reasoning sequence.

Our dynamic precision allocation adapts based on phase characteristics, reasoning progress, and confidence. The scheduler is guided by a principled linear model, which serves as a computationally efficient, first-order approximation of an ideal precision function. For a detailed justification, please see Appendix B. The model is defined as:

$$p_t = \max \left(p_{base}(\phi_t) - \alpha \cdot \frac{t}{T_{exp}} + \beta \cdot (1 - C(t)), 2 \right) \quad (5)$$

where $p_{base}(\phi_t)$ provides phase-specific baseline precision. T_{exp} is the expected number of reasoning thought and $\alpha \cdot \frac{t}{T_{exp}}$ implements progressive reduction aligned with reasoning advancement. $\beta \cdot (1 - C(t))$ increases precision when confidence is low. This formulation provides a robust and interpretable control strategy without the overhead of complex nonlinear models.

3.4 COORDINATED TERMINATION

Our termination strategy coordinates precision adaptation with stopping decisions through entropy-based confidence estimation computed from thought transition patterns. This coordination prevents precision-induced confidence degradation from causing suboptimal termination decisions.

For reasoning steps containing split tokens (in most cases also the important high-entropy tokens (Wang et al., 2025)) indicating reconsideration, we compute transition entropy as a measure of reasoning uncertainty:

$$H_t = - \sum_{v \in V_{split}} P(v|context_t) \log P(v|context_t) \quad (6)$$

where V_{split} contains transition vocabulary indicative of reasoning uncertainty and $P(v|context_t)$ represents the probability of generating transition token v given current reasoning context. Our unified confidence metric integrates phase-specific quality assessment with temporal confidence dynamics as:

$$C(t) = \omega_1 \cdot r_{\phi(s_t)} + \omega_2 \cdot \frac{H_{base} - H_t}{H_{base}} \quad (7)$$

270 where $r_{\phi(s_t)}$ represents phase-specific quality, and ω_i are weighting parameters. The coordinated
 271 termination decision integrates multiple criteria:
 272

$$\mathcal{T}(t) = (C(t) \geq \tau_e) \wedge (t \geq t_{min}) \quad (8)$$

274 where t_{min} enforces minimum number of thoughts and τ_e is the threshold. To implement natural
 275 termination, we employ confidence-based completion phrase injection. When termination criteria
 276 are satisfied, we append contextually appropriate completion indicators like “Okay, I think I have
 277 finished thinking” This approach maintains reasoning coherence while enabling efficient early exit.
 278

279 4 EXPERIMENTS

280 4.1 EXPERIMENTAL SETUP

283 **Models and Datasets.** We conduct comprehensive evaluation using two model variants: *DeepSeek-
 284 R1-Distill-Qwen-7B* (Guo et al., 2025) and *Qwen-3-8B* (Yang et al., 2025), implementing our frame-
 285 work with the Any-Precision quantization algorithm (Park et al., 2024) to enable seamless dynamic
 286 precision switching without memory overhead. To demonstrate TSAR’s applicability across different
 287 architectures. We evaluate performance on four challenging mathematical reasoning datasets that
 288 cover a wide spectrum of complexity: *GSM8K* (Cobbe et al., 2021), which consists of elementary-
 289 level word problems requiring sequential arithmetic reasoning; *MATH-500*, a high-difficulty subset
 290 of 500 competition-style problems derived from the *MATH* dataset; *AIME-120*, featuring problems
 291 from the American Invitational Mathematics Examination (2022–2025) that test advanced problem-
 292 solving techniques; and *AMC-23*, a selection of problems from the American Mathematics Com-
 293 petitions that assess deep conceptual understanding and strategic reasoning. In addition, we conducted
 294 evaluations on two general-purpose datasets: *GPQA-Diamond-MC* (Rein et al., 2024), a collec-
 295 tion of 198 highly challenging questions from the Graduate-Level Google-Proof Q&A benchmark;
 296 and *MMLU* (Hendrycks et al., 2021a), a benchmark spanning numerous academic and professional
 297 domains, designed to assess models’ general-purpose knowledge and reasoning capabilities.

298 **Baselines and Metrics.** We establish comprehensive baselines representing different optimization
 299 paradigms to evaluate TSAR’s effectiveness across multiple dimensions.

300 *Static Quantization Baselines.* We implement uniform quantization strategies where all reasoning
 301 phases operate at fixed precision levels: 3-bit uniform quantization and 4-bit uniform quantiza-
 302 tion (Frantar et al., 2022). These baselines represent conventional static approaches that cannot
 303 adapt to dynamic reasoning requirements.

304 *Adaptive Quantization Baseline.* Following the Progressive Mixed-Precision Decoding (PMPD)
 305 framework (Chen et al., 2025a), we implement a naive scheduler that switches from high-precision
 306 to low-precision models. This approach provides temporal adaptation without reasoning awareness,
 307 serving as a direct comparison for our coordinated strategy.

308 *Early Termination Baseline.* We compare our approach with two training-free early stopping meth-
 309 ods, *S1* length control (Muennighoff et al., 2025) and *NoThinking* (Ma et al., 2025a). In the compar-
 310 ison, we align their generation budgets with ours to enable a fair evaluation of performance.
 311

312 4.2 MAIN RESULTS

314 As presented in Table 1, TSAR demonstrates consistent and substantial superiority over all baselines
 315 across two distinct models and a wide spectrum of reasoning tasks. Our analysis is structured by
 316 task difficulty, revealing how TSAR’s coordinated optimization excels at every level of complexity.

317 **Dominant Efficiency on Foundational Reasoning Tasks (GSM8K).** On elementary mathemat-
 318 ical problems like *GSM8K*, where reasoning paths are relatively straightforward, TSAR delivers
 319 massive efficiency gains with virtually no accuracy trade-off. Across both models, it achieves a
 320 $5.7 \times$ - $6.2 \times$ *efficiency boost* while maintaining accuracy that is statistically indistinguishable from
 321 the full-precision baseline (e.g., 0.944 vs. 0.955 on *Qwen-3*). This performance highlights the ef-
 322 ficacy of our entropy-based termination criterion, which accurately detects the point of confidence
 323 saturation and prunes the redundant reasoning chain. In contrast, while *S1* length-control also re-
 duces tokens, its reliance on full precision makes it spatially inefficient (only $1.1 \times$ - $1.2 \times$ total gain).

324
325
326
Table 1: Model performance on various reasoning datasets. Efficiency is measured as a composite
of temporal and spatial efficiency.
327	328	329				330																																																																																																																																																																																																																																																																																																																																																																																																																																																																																																																																																																																																																																																																																																																																																																																																																																																																																																																																																																																																																																																																																																																																																																																																																																																																																																																																																																
331	332	333	334	335	336	337	338	339	340	341	342	343	344	345	346	347	348	349	350	351	352	353	354	355	356	357	358	359	360	361	362	363	364	365	366	367	368	369	370	371	372	373	374	375	376	377	378	379	380	381	382	383	384	385	386	387	388	389	390	391	392	393	394	395	396	397	398	399	400	401	402	403	404	405	406	407	408	409	410	411	412	413	414	415	416	417	418	419	420	421	422	423	424	425	426	427	428	429	430	431	432	433	434	435	436	437	438	439	440	441	442	443	444	445	446	447	448	449	450	451	452	453	454	455	456	457	458	459	460	461	462	463	464	465	466	467	468	469	470	471	472	473	474	475	476	477	478	479	480	481	482	483	484	485	486	487	488	489	490	491	492	493	494	495	496	497	498	499	500	501	502	503	504	505	506	507	508	509	510	511	512	513	514	515	516	517	518	519	520	521	522	523	524	525	526	527	528	529	530	531	532	533	534	535	536	537	538	539	540	541	542	543	544	545	546	547	548	549	550	551	552	553	554	555	556	557	558	559	560	561	562	563	564	565	566	567	568	569	570	571	572	573	574	575	576	577	578	579	580	581	582	583	584	585	586	587	588	589	590	591	592	593	594	595	596	597	598	599	600	601	602	603	604	605	606	607	608	609	610	611	612	613	614	615	616	617	618	619	620	621	622	623	624	625	626	627	628	629	630	631	632	633	634	635	636	637	638	639	640	641	642	643	644	645	646	647	648	649	650	651	652	653	654	655	656	657	658	659	660	661	662	663	664	665	666	667	668	669	670	671	672	673	674	675	676	677	678	679	680	681	682	683	684	685	686	687	688	689	690	691	692	693	694	695	696	697	698	699	700	701	702	703	704	705	706	707	708	709	710	711	712	713	714	715	716	717	718	719	720	721	722	723	724	725	726	727	728	729	730	731	732	733	734	735	736	737	738	739	740	741	742	743	744	745	746	747	748	749	750	751	752	753	754	755	756	757	758	759	760	761	762	763	764	765	766	767	768	769	770	771	772	773	774	775	776	777	778	779	780	781	782	783	784	785	786	787	788	789	790	791	792	793	794	795	796	797	798	799	800	801	802	803	804	805	806	807	808	809	810	811	812	813	814	815	816	817	818	819	820	821	822	823	824	825	826	827	828	829	830	831	832	833	834	835	836	837	838	839	840	841	842	843	844	845	846	847	848	849	850	851	852	853	854	855	856	857	858	859	860	861	862	863	864	865	866	867	868	869	870	871	872	873	874	875	876	877	878	879	880	881	882	883	884	885	886	887	888	889	890	891	892	893	894	895	896	897	898	899	900	901	902	903	904	905	906	907	908	909	910	911	912	913	914	915	916	917	918	919	920	921	922	923	924	925	926	927	928	929	930	931	932	933	934	935	936	937	938	939	940	941	942	943	944	945	946	947	948	949	950	951	952	953	954	955	956	957	958	959	960	961	962	963	964	965	966	967	968	969	970	971	972	973	974	975	976	977	978	979	980	981	982	983	984	985	986	987	988	989	990	991	992	993	994	995	996	997	998	999	1000	1001	1002	1003	1004	1005	1006	1007	1008	1009	1010	1011	1012	1013	1014	1015	1016	1017	1018	1019	1020	1021	1022	1023	1024	1025	1026	1027	1028	1029	1030	1031	1032	1033	1034	1035	1036	1037	1038	1039	1040	1041	1042	1043	1044	1045	1046	1047	1048	1049	1050	1051	1052	1053	1054	1055	1056	1057	1058	1059	1060	1061	1062	1063	1064	1065	1066	1067	1068	1069	1070	1071	1072	1073	1074	1075	1076	1077	1078	1079	1080	1081	1082	1083	1084	1085	1086	1087	1088	1089	1090	1091	1092	1093	1094	1095	1096	1097	1098	1099	1100	1101	1102	1103	1104	1105	1106	1107	1108	1109	1110	1111	1112	1113	1114	1115	1116	1117	1118	1119	1120	1121	1122	1123	1124	1125	1126	1127	1128	1129	1130	1131	1132	1133	1134	1135	1136	1137	1138	1139	1140	1141	1142	1143	1144	1145	1146	1147	1148	1149	1150	1151	1152	1153	1154	1155	1156	1157	1158	1159	1160	1161	1162	1163	1164	1165	1166	1167	1168	1169	1170	1171	1172	1173	1174	1175	1176	1177	1178	1179	1180	1181	1182	1183	1184	1185	1186	1187	1188	1189	1190	1191	1192	1193	1194	1195	1196	1197	1198	1199	1200	1201	1202	1203	1204	1205	1206	1207	1208	1209	1210	1211	1212	1213	1214	1215	1216	1217	1218	1219	1220	1221	1222	1223	1224	1225	1226	1227	1228	1229	1230	1231	1232	1233	1234	1235	1236	1237	1238	1239	1240	1241	1242	1243	1244	1245	1246	1247	1248	1249	1250	1251	1252	1253	1254	1255	1256	1257	1258	1259	1260	1261	1262	1263	1264	1265	1266	1267	1268	1269	1270	1271	1272	1273	1274	1275	1276	1277	1278	1279	1280	1281	1282	1283	1284	1285	1286	1287	1288	1289	1290	1291	1292	1293	1294	1295	1296	1297	1298	1299	1300	1301	1302	1303	1304	1305	1306	1307	1308	1309	1310	1311	1312	1313	1314	1315	1316	1317	1318	1319	1320	1321	1322	1323	1324	1325	1326	1327	1328	1329	1330	1331	1332	1333	1334	1335	1336	1337	1338	1339	1340	1341	1342	1343	1344	1345	1346	1347	1348	1349	1350	1351	1352	1353	1354	1355	1356	1357	1358	1359	1360	1361	1362	1363	1364	1365	1366	1367	1368	1369	1370	1371	1372	1373	1374	1375	1376	1377	1378	1379	1380	1381	1382	1383	1384	1385	1386	1387	1388	1389	1390	1391	1392	1393	1394	1395	1396	1397	1398	1399	1400	1401	1402	1403	1404	1405	1406	1407	1408	1409	1410	1411	1412	1413	1414	1415	1416	1417	1418	1419	1420	1421	1422	1423	1424	1425	1426	1427	1428	1429	1430	1431	1432	1433	1434	1435	1436	1437	1438	1439	1440	1441	1442	1443	1444	1445	1446	1447	1448	1449	1450	1451	1452	1453	1454	1455	1456	1457	1458	1459	1460	1461	1462	1463	1464	1465	1466	1467	1468	1469	1470	1471	1472	1473	1474	1475	1476	1477	1478	1479	1480	1481	1482	1483	1484	1485	1486	1487	1488	1489	1490	1491	1492	1493	1494	1495	1496	1497	1498	1499	1500	1501	1502	1503	1504	1505	1506	1507	1508	1509	1510	1511	1512	1513	1514	1515	1516	1517	1518	1519	1520	1521	1522	1523	1524	1525	1526	1527	1528	1529	1530	1531	1532	1533	1534	1535	1536	1537	1538	1539	1540	1541	1542	1543	1544	1545	1546	1547	1548	1549	1550	1551	1552	1553	1554	1555	1556	1557	1558	1559	1560	1561	1562	1563	1564	1565	1566	1567	1568	1569	1570	1571	1572	1573	1574	1575	1576	1577	1578	1579	1580	1581	1582	1583	1584	1585	1586	1587	1588	1589	1590	1591	1592	1593	1594	1595	1596	1597	1598	1599	1600	1601	1602	1603	1604	1605	1606	1607	1608	1609	1610	1611	1612	1613	1614	1615	1616	1617	1618	1619	1620	1621	1622	1623	1624	1625	1626	1627	1628	1629	1630	1631	1632	1633	1634	1635	1636	1637	1638	1639	1640	1641	1642	1643	1644	1645	1646	1647	1648	1

378 proves its ability to navigate this trade-off effectively. It retains over *97% of the original accuracy*
 379 on both models (99.1% for DeepSeek-R1, 97.7% for Qwen-3) while delivering a $5.3 \times$ – $6.2 \times$ effi-
 380 ciency gain. This success is directly attributable to our phase-aware scheduling. The framework
 381 allocates higher precision to critical initial phases, then progressively reduces it, preventing the kind
 382 of catastrophic errors seen in baselines. For instance, the PMPD scheduler, with its one-way switch
 383 from high to low precision, is too brittle for this complexity, causing a *severe 11.2% accuracy drop*
 384 on DeepSeek-R1. Under comparable token counts relative to TSAR while preserving their original
 385 precision, both S1 length-control and the NoThinking method demonstrate unstable accuracy at an
 386 efficiency ratio of $1.1 \times$ – $1.5 \times$, significantly underperforming compared to our method. This demon-
 387 strates that as problems become harder, a simple temporal schedule is insufficient; a coordinated,
 388 context-aware strategy like TSAR’s is required to succeed.
 389

390 **Robustness Under Pressure in Contest-Level Scenarios (AIME-120, AMC-23).** The superior-
 391 ity of TSAR is most pronounced on high-difficulty contest benchmarks, where baseline methods
 392 often collapse. On AIME-120, TSAR preserves an impressive 85.1% (*DeepSeek-R1*) and 93.8%
 393 (*Qwen-3*) of *original accuracy* with over $6 \times$ efficiency. On AMC-23, TSAR also achieve an effi-
 394 ciency gain of $6.5 \times$ – $7.4 \times$. PMPD’s performance, however, plummets, demonstrating its inability
 395 to handle sophisticated reasoning under compression. These findings strongly validate that our co-
 396 ordinated, phase-aware optimization is not merely beneficial but *essential* for preserving reasoning
 397 capabilities in the most demanding scenarios.
 398

399 **Broad Applicability on General-Purpose Reasoning (MMLU, GPQA-Diamond-MC).** To con-
 400 firm that TSAR’s benefits extend beyond mathematical domains, we evaluated it on the multi-
 401 domain MMLU benchmark. The results affirm its broad applicability. TSAR again achieves a *high*
 402 *efficiency gain* ($5.6 \times$ – $7.0 \times$) while matching the original model’s accuracy (e.g., 0.633 vs. 0.634
 403 on DeepSeek-R1; 0.823 vs. 0.826 on Qwen-3). Similarly, on the challenging GPQA-Diamond-
 404 MC dataset, TSAR opens up a significant accuracy gap of up to *6.5% over PMPD, 7.1% over S1*
 405 *and 13.1% over NoThinking* (on DeepSeek-R1). Our method achieves a significant improvement
 406 in both accuracy and efficiency, despite operating at comparable precision to PMPD and similar to-
 407 ken counts to S1 length-control and the NoThinking. Although Uniform 3-bit quantization attains
 408 the best efficiency on the Qwen-3-8B model, its considerable loss in accuracy cannot be overlooked.
 409 This demonstrates that TSAR’s principles of identifying and exploiting temporal-spatial redundancy
 410 are task-agnostic and highly effective for general-purpose reasoning as well.
 411

4.3 ABLATION STUDY

412 We conducted systematic ablation studies to
 413 evaluate the impact of each TSAR component
 414 by progressively reducing its parameter val-
 415 ues to 0 while keeping other components fixed.
 416 Using the MATH-500 benchmark, we mea-
 417 sured performance through two key metrics: (1)
 418 per-question average token count (indicative of
 419 computational efficiency) and (2) dataset-wide
 420 accuracy (reflecting overall task performance).
 421 As detailed in Table 2, The study reveals three key results:

Table 2: Ablation Study Results.

ω_1	0	0.1	0.2	0.3	0.4	0.5
Accuracy	0.904	0.904	0.906	0.910	0.916	0.924
Avg. Tokens	2651.23	2690.37	2715.69	2954.88	3242.13	3460.92
ω_2	0	0.1	0.2	0.3	0.4	0.5
Accuracy	0.934	0.926	0.920	0.914	0.908	0.906
Avg. Tokens	4232.07	3369.71	3028.56	2936.48	2869.32	2806.09
t_{\min}	0	1	2	3	4	5
Accuracy	0.914	0.922	0.920	0.922	0.926	0.932
Avg. Tokens	2762.35	2993.74	3243.45	3410.62	3784.10	3915.86

422 • *Ablation of phase quality weight:* By gradually reducing ω_1 to 0, we observe that the
 423 accuracy first drops rapidly before stabilizing at 0.904, while the token count decreases
 424 sharply and then plateaus around 2,600 tokens.
 425

426 • *Ablation of entropy shift weight:* Similarly, when reducing ω_2 to 0, the reasoning sequence
 427 s loses its constraints. Consequently, the truncation point of our method depends solely
 428 on textual phrasing, leading to a gradual increase in both token count and accuracy. This
 429 clearly demonstrates TSAR’s superior capability in dynamically adjusting token allocation
 430 based on problem difficulty.
 431

• *Ablation of reasoning window:* As t_{\min} is progressively reduced to 0, the robustness of our
 method declines. Intuitively, early exits may occur at suboptimal points due to inflated

432 confidence values. Correspondingly, we observe a consistent decrease in both token count
 433 and accuracy.
 434

435 4.4 LATENCY ANALYSIS

436 We evaluate inference latency following the methodology of PMPD
 437 (Chen et al., 2025a), reporting *per-task latency* (average seconds per
 438 question) to enable direct comparison across methods. Unlike end-to-end
 439 dataset latency measurements common in some works, per-task latency isolates hardware efficiency from dataset size variations.
 440

Table 3: Per-task latency (seconds) and token counts across different datasets for DeepSeek-R1-Distill-Qwen-7B.

Method	GSM8K		MATH-500		AIME120		GPQA		AMC23	
	Lat.	Tok.	Lat.	Tok.	Lat.	Tok.	Lat.	Tok.	Lat.	Tok.
16-bit	21.3	1847	40.1	4187	146.7	14910	91.6	9850	67.8	6855
4-bit	13.3	1822	25.0	4460	89.8	14141	46.2	8769	42.4	6660
3-bit	9.6	1858	18.1	4223	61.4	12481	33.8	8123	30.7	7929
TSAR	6.7	1354	13.6	2994	48.7	9900	15.6	3762	22.4	4643

441 The results are shown in Table 3. While static quantization at 4-bit and 3-bit precision is expectedly
 442 to reduce latency compared to the 16-bit original, our TSAR framework demonstrates substantially
 443 greater gains. Specifically, TSAR achieves speedups ranging from $2.9\times$ to $5.9\times$ across various
 444 datasets. Moreover, it attains higher accuracy (as shown in Table 1) than the Uniform 3-bit model
 445 while simultaneously achieving lower latency, indicating that TSAR realizes an optimal trade-off
 446 between performance and efficiency.
 447

451 5 RELATED WORK

452 **CoT Reasoning Efficiency.** Recent efforts to improve CoT reasoning efficiency focus on token
 453 reduction by shortening CoT paths, building smaller models, or accelerating decoding (Feng et al.,
 454 2025; Hashemi et al., 2025; Chen et al., 2024; Lee et al., 2025). Methods to shorten CoT chains
 455 include training-dependent approaches like reinforcement learning (RL) with length penalties (Ma
 456 et al., 2025b; Li et al., 2025; Aggarwal & Welleck, 2025; Xia et al., 2025; Hou et al., 2025) (e.g.,
 457 O1-Pruner (Luo et al., 2025), DAST (Shen et al., 2025a)) and supervised fine-tuning (SFT) on
 458 variable-length data (Xia et al., 2025; Ma et al., 2025b). Training-free alternatives use prompting
 459 to enforce brevity or route queries to specialized models (Renze & Guven, 2024; Ong et al., 2024).
 460 Other strategies build smaller, more capable models via knowledge distillation (Feng et al., 2024;
 461 Chen et al., 2025b; Shen et al., 2025b) or accelerate decoding with techniques like problem decom-
 462 position (Teng et al., 2025) and speculative decoding (Pan et al., 2025). These approaches often
 463 require training or treating redundancy dimensions independently, overlooking phase-specific pat-
 464 terns. Unlike them, our TSAR framework provides training-free, phase-aware joint optimization of
 465 temporal and spatial redundancy.
 466

467 **LLM Efficiency.** Model compression is pivotal for alleviating the high resource demands of
 468 LLMs, with key strategies including knowledge distillation (Gou et al., 2021), pruning (Frantar &
 469 Alistarh, 2023), and quantization (Lin et al., 2024; Frantar et al., 2022). Among these, post-training
 470 quantization (PTQ) provides a practical option by compressing models after training while retaining
 471 most performance with low overhead. Recent PTQ innovations include SmoothQuant (Xiao et al.,
 472 2023), which handles activation outliers for smoother low-bit conversion; GPTQ (Frantar et al.,
 473 2022), which fine-tunes quantization layer by layer; and AWQ (Lin et al., 2024), which prioritizes
 474 salient weights to maintain generation quality. Versatile systems like Any-Precision LLM (Park
 475 et al., 2024) allow runtime selection of bit-widths from a single model without added storage costs,
 476 and Progressive Mixed-Precision Decoding (Chen et al., 2025a) varies precision adaptively through-
 477 out the decoding sequence. Despite their effectiveness in curbing spatial overhead, these methods
 478 typically enforce broad, non-specialized policies that disregard the varying demands of CoT phases.
 479

480 6 CONCLUSION

481 We presented TSAR, a training-free framework for optimizing Chain-of-Thought reasoning through
 482 coordinated temporal and spatial redundancy exploitation. Our approach achieves up to $12.4\times$
 483 speedup while maintaining accuracy without requiring training. The results establish coordinated
 484 multi-dimensional optimization as substantially superior to conventional strategies, opening new
 485 directions for practical reasoning optimization.

486
487 ETHICS STATEMENT488 Our work focuses on enhancing the computational efficiency of LLM reasoning using public models
489 and benchmarks. By dynamically adjusting computational precision and stopping criteria without
490 altering model parameters, our method introduces no new ethical risks and inherits the profile of the
491 base models. This approach aims to democratize access to advanced AI for resource-constrained
492 environments and reduce the environmental footprint of LLM deployments.493
494 REPRODUCIBILITY STATEMENT495 Our experiments are conducted on public models and benchmarks. For all reported results, we
496 average four runs with different random seeds; the main experiments use a fixed seed (42) for direct
497 replication. We will open-source our complete implementation to ensure full reproducibility and
498 facilitate future research.500
501 REFERENCES502 Pranjal Aggarwal and Sean Welleck. L1: Controlling how long a reasoning model thinks with
503 reinforcement learning. *arXiv preprint arXiv:2503.04697*, 2025.504
505 Hao (Mark) Chen, Fuwen Tan, Alexandros Kouris, Roysen Lee, Hongxiang Fan, and Stylianos I.
506 Venieris. Progressive Mixed-Precision Decoding for Efficient LLM Inference. In *International
507 Conference on Learning Representations (ICLR)*, 2025a.508
509 Xinghao Chen, Zhijing Sun, Wenjin Guo, Miaoran Zhang, Yanjun Chen, Yirong Sun, Hui Su, Yijie
510 Pan, Dietrich Klakow, Wenjie Li, et al. Unveiling the key factors for distilling chain-of-thought
511 reasoning. *arXiv preprint arXiv:2502.18001*, 2025b.512
513 Xingyu Chen, Jiahao Xu, Tian Liang, Zhiwei He, Jianhui Pang, Dian Yu, Linfeng Song, Qiuzhi Liu,
514 Mengfei Zhou, Zhuosheng Zhang, et al. Do not think that much for 2+ 3=? on the overthinking
515 of o1-like llms. *arXiv preprint arXiv:2412.21187*, 2024.516
517 Karl Cobbe, Vineet Kosaraju, Mohammad Bavarian, Mark Chen, Heewoo Jun, Lukasz Kaiser,
518 Matthias Plappert, Jerry Tworek, Jacob Hilton, Reiichiro Nakano, et al. Training verifiers to
519 solve math word problems. *arXiv preprint arXiv:2110.14168*, 2021.520 John Dewey. *How we think*. Houghton Mifflin, 1933.521
522 Sicheng Feng, Gongfan Fang, Xinyin Ma, and Xinchao Wang. Efficient reasoning models: A survey.
523 *arXiv preprint arXiv:2504.10903*, 2025.524
525 Tao Feng, Yicheng Li, Li Chenglin, Hao Chen, Fei Yu, and Yin Zhang. Teaching small language
526 models reasoning through counterfactual distillation. 2024.527
528 Elias Frantar and Dan Alistarh. Sparsegpt: Massive language models can be accurately pruned in
529 one-shot. In *International Conference on Machine Learning*, pp. 10323–10337. PMLR, 2023.530
531 Elias Frantar, Saleh Ashkboos, Torsten Hoefler, and Dan Alistarh. Gptq: Accurate post-training
532 quantization for generative pre-trained transformers. *arXiv preprint arXiv:2210.17323*, 2022.533
534 Jianping Gou, Baosheng Yu, Stephen J Maybank, and Dacheng Tao. Knowledge distillation: A
535 survey. *International Journal of Computer Vision*, 129(6):1789–1819, 2021.536
537 Daya Guo, Dejian Yang, Haowei Zhang, Junxiao Song, Ruoyu Zhang, Runxin Xu, Qihao Zhu,
538 Shirong Ma, Peiyi Wang, Xiao Bi, et al. Deepseek-r1: Incentivizing reasoning capability in llms
539 via reinforcement learning. *arXiv preprint arXiv:2501.12948*, 2025.540
541 Masoud Hashemi, Oluwanifemi Bambose, Sathwik Tejaswi Madhusudhan, Jishnu Sethumadhavan
542 Nair, Aman Tiwari, and Vikas Yadav. Dnr bench: Benchmarking over-reasoning in reasoning
543 llms. *arXiv preprint arXiv:2503.15793*, 2025.

540 Dan Hendrycks, Collin Burns, Steven Basart, Andy Zou, Mantas Mazeika, Dawn Song, and Ja-
 541 cob Steinhardt. Measuring massive multitask language understanding, 2021a. URL <https://arxiv.org/abs/2009.03300>.

542

543 Dan Hendrycks, Collin Burns, Saurav Kadavath, Akul Arora, Steven Basart, Eric Tang, Dawn Song,
 544 and Jacob Steinhardt. Measuring mathematical problem solving with the math dataset. *arXiv*
 545 *preprint arXiv:2103.03874*, 2021b.

546

547 Bairu Hou, Yang Zhang, Jiabao Ji, Yujian Liu, Kaizhi Qian, Jacob Andreas, and Shiyu Chang.
 548 Thinkprune: Pruning long chain-of-thought of llms via reinforcement learning. *arXiv preprint*
 549 *arXiv:2504.01296*, 2025.

550

551 Yu Kang, Xianghui Sun, Liangyu Chen, and Wei Zou. C3ot: Generating shorter chain-of-thought
 552 without compromising effectiveness. *arXiv preprint arXiv:2412.11664*, 2024.

553

554 Ayeong Lee, Ethan Che, and Tianyi Peng. How well do llms compress their own chain-of-thought?
 555 a token complexity approach. *arXiv preprint arXiv:2503.01141*, 2025.

556

557 Chen Li, Nazhou Liu, and Kai Yang. Adaptive group policy optimization: Towards stable training
 558 and token-efficient reasoning. *arXiv preprint arXiv:2503.15952*, 2025.

559

560 Yiwei Li, Peiwen Yuan, Shaoxiong Feng, Boyuan Pan, Xinglin Wang, Bin Sun, Heda Wang, and
 561 Kan Li. Escape sky-high cost: Early-stopping self-consistency for multi-step reasoning. *arXiv*
 562 *preprint arXiv:2401.10480*, 2024.

563

564 Ji Lin, Jiaming Tang, Haotian Tang, Shang Yang, Wei-Ming Chen, Wei-Chen Wang, Guangxuan
 565 Xiao, Xingyu Dang, Chuang Gan, and Song Han. Awq: Activation-aware weight quantization for
 566 on-device llm compression and acceleration. *Proceedings of Machine Learning and Systems*, 6:
 567 87–100, 2024.

568

569 Tengxiao Liu, Qipeng Guo, Xiangkun Hu, Cheng Jiayang, Yue Zhang, Xipeng Qiu, and Zheng
 570 Zhang. Can language models learn to skip steps? *arXiv preprint arXiv:2411.01855*, 2024.

571

572 Haotian Luo, Li Shen, Haiying He, Yibo Wang, Shiwei Liu, Wei Li, Naiqiang Tan, Xiaochun Cao,
 573 and Dacheng Tao. O1-pruner: Length-harmonizing fine-tuning for o1-like reasoning pruning.
 574 *arXiv preprint arXiv:2501.12570*, 2025.

575

576 Wenjie Ma, Jingxuan He, Charlie Snell, Tyler Griggs, Sewon Min, and Matei Zaharia. Reasoning
 577 models can be effective without thinking, 2025a. URL <https://arxiv.org/abs/2504.09858>.

578

579 Xinyin Ma, Guangnian Wan, Runpeng Yu, Gongfan Fang, and Xinchao Wang. Cot-valve: Length-
 580 compressible chain-of-thought tuning. *arXiv preprint arXiv:2502.09601*, 2025b.

581

582 Niklas Muennighoff, Zitong Yang, Weijia Shi, Xiang Lisa Li, Li Fei-Fei, Hannaneh Hajishirzi, Luke
 583 Zettlemoyer, Percy Liang, Emmanuel Candès, and Tatsunori Hashimoto. s1: Simple test-time
 584 scaling. *arXiv preprint arXiv:2501.19393*, 2025.

585

586 Isaac Ong, Amjad Almahairi, Vincent Wu, Wei-Lin Chiang, Tianhao Wu, Joseph E Gonzalez,
 587 M Waleed Kadous, and Ion Stoica. Routellm: Learning to route llms with preference data. *arXiv*
 588 *preprint arXiv:2406.18665*, 2024.

589

590 Rui Pan, Yinwei Dai, Zhihao Zhang, Gabriele Oliaro, Zhihao Jia, and Ravi Netravali. Specrea-
 591 son: Fast and accurate inference-time compute via speculative reasoning. *arXiv preprint*
 592 *arXiv:2504.07891*, 2025.

593

594 Shubham Parashar, Blake Olson, Sambhav Khurana, Eric Li, Hongyi Ling, James Caverlee, and
 595 Shuiwang Ji. Inference-time computations for llm reasoning and planning: A benchmark and
 596 insights. *arXiv preprint arXiv:2502.12521*, 2025.

597

598 Yeonhong Park, Jake Hyun, SangLyul Cho, Bonggeun Sim, and Jae W Lee. Any-precision llm:
 599 Low-cost deployment of multiple, different-sized llms. *arXiv preprint arXiv:2402.10517*, 2024.

594 Ziqing Qiao, Yongheng Deng, Jiali Zeng, Dong Wang, Lai Wei, Fandong Meng, Jie Zhou, Ju Ren,
 595 and Yaoxue Zhang. Concise: Confidence-guided compression in step-by-step efficient reasoning.
 596 *arXiv preprint arXiv:2505.04881*, 2025.

597

598 David Rein, Betty Li Hou, Asa Cooper Stickland, Jackson Petty, Richard Yuanzhe Pang, Julien Di-
 599 rani, Julian Michael, and Samuel R Bowman. Gpqa: A graduate-level google-proof q&a bench-
 600 mark. In *First Conference on Language Modeling*, 2024.

601 Matthew Renze and Erhan Guven. The benefits of a concise chain of thought on problem-solving in
 602 large language models. In *FLLM*, 2024.

603

604 Yi Shen, Jian Zhang, Jieyun Huang, Shuming Shi, Wenjing Zhang, Jiangze Yan, Ning Wang, Kai
 605 Wang, and Shiguo Lian. Dast: Difficulty-adaptive slow-thinking for large reasoning models.
 606 *arXiv preprint arXiv:2503.04472*, 2025a.

607 Zhenyi Shen, Hanqi Yan, Linhai Zhang, Zhanghao Hu, Yali Du, and Yulan He. Codi: Compressing
 608 chain-of-thought into continuous space via self-distillation. *arXiv preprint arXiv:2502.21074*,
 609 2025b.

610 Yang Sui, Yu-Neng Chuang, Guanchu Wang, Jiamu Zhang, Tianyi Zhang, Jiayi Yuan, Hongyi Liu,
 611 Andrew Wen, Shaochen Zhong, Hanjie Chen, et al. Stop overthinking: A survey on efficient
 612 reasoning for large language models. *arXiv preprint arXiv:2503.16419*, 2025.

613

614 Fengwei Teng, Zhaoyang Yu, Quan Shi, Jiayi Zhang, Chenglin Wu, and Yuyu Luo. Atom of thoughts
 615 for markov llm test-time scaling. *arXiv preprint arXiv:2502.12018*, 2025.

616 Shenzhi Wang, Le Yu, Chang Gao, Chujie Zheng, Shixuan Liu, Rui Lu, Kai Dang, Xionghui Chen,
 617 Jianxin Yang, Zhenru Zhang, et al. Beyond the 80/20 rule: High-entropy minority tokens drive
 618 effective reinforcement learning for llm reasoning. *arXiv preprint arXiv:2506.01939*, 2025.

619

620 Jason Wei, Xuezhi Wang, Dale Schuurmans, Maarten Bosma, Fei Xia, Ed Chi, Quoc V Le, Denny
 621 Zhou, et al. Chain-of-thought prompting elicits reasoning in large language models. 2022.

622 Heming Xia, Yongqi Li, Chak Tou Leong, Wenjie Wang, and Wenjie Li. Tokenskip: Controllable
 623 chain-of-thought compression in llms. *arXiv preprint arXiv:2502.12067*, 2025.

624

625 Guangxuan Xiao, Ji Lin, Mickael Seznec, Hao Wu, Julien Demouth, and Song Han. Smoothquant:
 626 Accurate and efficient post-training quantization for large language models. In *International
 627 Conference on Machine Learning*, pp. 38087–38099. PMLR, 2023.

628

629 An Yang, Beichen Zhang, Binyuan Hui, Bofei Gao, Bowen Yu, Chengpeng Li, Dayiheng Liu,
 630 Jianhong Tu, Jingren Zhou, Junyang Lin, Keming Lu, Mingfeng Xue, Runji Lin, Tianyu Liu,
 631 Xingzhang Ren, and Zhenru Zhang. Qwen2.5-math technical report: Toward mathematical ex-
 632 pert model via self-improvement, 2024. URL <https://arxiv.org/abs/2409.12122>.

633

634 An Yang, Anfeng Li, Baosong Yang, Beichen Zhang, Binyuan Hui, Bo Zheng, Bowen Yu,
 635 Chang Gao, Chengen Huang, Chenxu Lv, et al. Qwen3 technical report. *arXiv preprint
 636 arXiv:2505.09388*, 2025.

637

638 Nan Zhang, Yusen Zhang, Prasenjit Mitra, and Rui Zhang. When reasoning meets compression:
 639 Benchmarking compressed large reasoning models on complex reasoning tasks. *arXiv preprint
 640 arXiv:2504.02010*, 2025.

641

642

643

644

645

646

647

648	APPENDIX	
649		
650	A The Use of Large Language Models (LLMs)	S2
651		
652	B Justification for Equation (5)	S2
653		
654	B.1 Theoretical Foundation	S2
655		
656	B.2 Mapping to the TSAR Scheduler	S2
657		
658	C TSAR Algorithm	S3
659		
660	D Details of Reasoning Phrase Classification	S3
661		
662	E Completion Indicators	S4
663		
664	F Case Study	S5
665		
666		
667		
668		
669		
670		
671		
672		
673		
674		
675		
676		
677		
678		
679		
680		
681		
682		
683		
684		
685		
686		
687		
688		
689		
690		
691		
692		
693		
694		
695		
696		
697		
698		
699		
700		
701		

702 A THE USE OF LARGE LANGUAGE MODELS (LLMs)

704 During the writing process, we utilized LLMs, specifically GPT-5, to refine the manuscript's lan-
 705 guage for clarity and fluency. The authors retained full responsibility for all content, with the LLMs
 706 serving exclusively as a tool for language enhancement.

708 B JUSTIFICATION FOR EQUATION (5)

710 The linear structure of our dynamic precision scheduler in Equation 5 is grounded in a first-order
 711 Taylor approximation of an optimal, yet intractable, precision function.

713 B.1 THEORETICAL FOUNDATION

715 Let us assume there exists an ideal precision function $p^* = f(t, C)$ that perfectly maps the reasoning
 716 progress (time step t) and the model's current confidence (C) to the optimal number of bits. This
 717 function is complex and unknown. To create a practical scheduler, we can approximate it using a
 718 first-order Taylor expansion around a specific operational point (t_0, C_0) :

$$720 \quad p^* \approx f(t_0, C_0) + \frac{\partial f}{\partial t} \Big|_{(t_0, C_0)} (t - t_0) + \frac{\partial f}{\partial C} \Big|_{(t_0, C_0)} (C - C_0) \quad (9)$$

722 We define our operational point at the start of a reasoning phase, where progress $t_0 = 0$. For the
 723 initial confidence C_0 , we make a foundational definition. At $t = 0$, the reasoning process has not
 724 yet begun, meaning no computational steps have been taken and, therefore, no uncertainty or error
 725 has been introduced. The concept of "measured confidence" is not yet applicable. We thus define
 726 the confidence at this boundary condition to be $C_0 = 1$, representing an idealized state of zero
 727 uncertainty before the first computational step.

729 B.2 MAPPING TO THE TSAR SCHEDULER

731 Our proposed scheduler is a direct, practical implementation of Equation 9. We map each term as
 732 follows:

- 733 • **Zeroth-Order Term:** The value of the function at the operational point, $f(0, 1)$, represents
 734 the optimal precision at the beginning of a phase with perfect confidence. This is naturally
 735 modeled by our phase-specific baseline:

$$737 \quad f(0, 1) \triangleq p_{base}(\phi_t) \quad (10)$$

- 739 • **First-Order Term (Progress):** The term $\frac{\partial f}{\partial t} \Big|_{(0,1)} \cdot t$ captures how precision should change
 740 with time. Based on our empirical observations, initial reasoning steps are more critical,
 741 implying that the required precision decreases as reasoning progresses. We therefore model
 742 the partial derivative as a negative constant:

$$743 \quad \frac{\partial f}{\partial t} \Big|_{(0,1)} \triangleq -\frac{\alpha}{T_{exp}} \quad (11)$$

746 This leads to the term $-\alpha \cdot \frac{t}{T_{exp}}$ in our scheduler.

- 748 • **First-Order Term (Confidence):** The term $\frac{\partial f}{\partial C} \Big|_{(0,1)} \cdot (C - 1)$ captures how precision
 749 should adapt to changes in confidence. Intuitively, a drop in confidence requires an increase
 750 in precision to mitigate potential errors. This implies an inverse relationship, so we model
 751 this partial derivative as a different negative constant:

$$752 \quad \frac{\partial f}{\partial C} \Big|_{(0,1)} \triangleq -\beta \quad (12)$$

755 Substituting this into the Taylor expansion gives the term $-\beta(C - 1)$, which is algebraically
 equivalent to $+\beta(1 - C)$ as used in our scheduler.

756 By combining these components, our scheduler from Equation 5 emerges as a direct implementation
 757 of the first-order approximation:
 758

$$p_t \approx p_{base}(\phi_t) - \alpha \cdot \frac{t}{T_{exp}} + \beta \cdot (1 - C(t)) \quad (13)$$

761 This principled approach provides a justification for the linear form of our scheduler, demonstrating
 762 that it is a well-founded design choice balancing accuracy and computational efficiency.
 763

764 **Algorithm 1** TSAR: Temporal-Spatial Adaptive Reasoning

765 **Require:** Reasoning LLM M , \mathbf{x} , thresholds $\{\tau_u, \tau_e\}$, weights $\{\alpha, \beta\}$
 766 **Ensure:** Generate sequence \mathbf{s} , precision \mathbf{p}

767 1: $p_0 \leftarrow 4$, $t \leftarrow 0$, $N_{adapt} \leftarrow 0$, $H_{conf} \leftarrow []$
 768 2: **while** $t < T_{max}$ **and not** terminated **do**
 769 3: $s_{t+1} \leftarrow M(s_{1:t}, p_t)$
 770 4: $H_{conf}.append(C_{base}(s_{t+1}))$
 771 5: **if** $S(s_{t+1})$ **then**
 772 6: $\phi_{t+1} \leftarrow \Phi(s_{t+1})$
 773 7: $H_t \leftarrow \text{ComputeEntropy}(s_{t+1})$
 774 8: $S_t \leftarrow \text{AssessStability}(H_{conf})$
 775 9: $C_t \leftarrow \text{UnifiedConfidence}(\phi_{t+1}, H_t, S_t)$
 776 10: $prog \leftarrow t/T_{exp}$
 777 11: $p_{target} \leftarrow \max(p_{base}(\phi_{t+1}) - \alpha \cdot prog - \beta \cdot (1 - C_t) - \gamma \cdot U(\phi_{t+1}), 2)$
 778 12: **if** $C_t \geq \tau_p$ **and** $p_t > p_{target}$ **then**
 779 13: $p_{t+1} \leftarrow p_{target}$, $N_{adapt} \leftarrow N_{adapt} + 1$
 780 14: ExecuteAdaptation(Δt)
 781 15: **else**
 782 16: $p_{t+1} \leftarrow p_t$
 783 17: **end if**
 784 18: **if** $C_t \geq \tau_e$ **and** S_t **and** $\mathcal{PC}(\phi_{t+1})$ **and** $t \geq t_{min}$ **then**
 785 19: InjectCompletion(ϕ_{t+1})
 786 20: **return** $\mathbf{s}_{1:t+1}$, $\mathbf{p}_{1:t+1}$
 21: **end if**
 787 22: **else**
 788 23: $p_{t+1} \leftarrow p_t$
 789 24: **end if**
 790 25: $t \leftarrow t + 1$
 791 26: **end while**
 792 27: **return** $\mathbf{s}_{1:t}$, $\mathbf{p}_{1:t}$

793
 794 **C TSAR ALGORITHM**

795 Algorithm 1 presents our TSAR framework. The algorithm operates by monitoring reasoning gen-
 796 eration for thought transition points, which serve as coordination opportunities. At each transition,
 797 it performs phase classification, computes unified confidence metrics, and makes coordinated deci-
 798 sions about precision adaptation and potential termination.
 799

800
 801 **D DETAILS OF REASONING PHRASE CLASSIFICATION**

802 To understand the internal mechanics of TSAR, we analyze two key components: the accuracy of
 803 our phase classifier and the resulting dynamic precision allocation strategy. The effectiveness of
 804 our framework hinges on correctly identifying the current reasoning phase to apply the appropriate
 805 optimization policy. As shown in Figure 1, our lightweight, keyword-based phase classifier (Eq.
 806 (5)) achieves nearly 90% average accuracy (details of this classifier can be found in Table 1). While
 807 this keyword-based classifier demonstrates high accuracy and efficiency for the tasks evaluated, we
 808 acknowledge that its robustness may vary on out-of-domain problems. Future work could explore
 809

Table 1: Keywords used in reasoning phrase classification.

Phase	Keywords
PF	recall, define, since, condition, theorem, inequality
SC	compute, calculate, formula, integral, \int , $=$, $+$, $-$, $*$, $/$, $\sqrt{}$, sin, cos, [
SV	check, verify, inconsistent, actually, hold on, error, doubt, ?, how, whether, confirm, correct

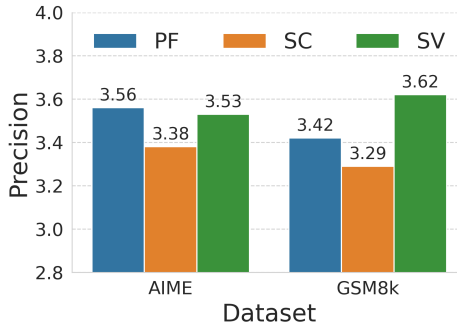
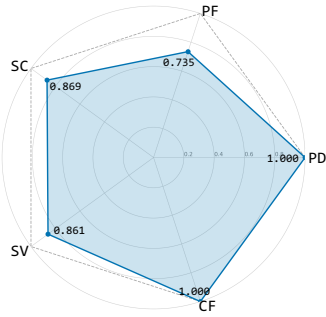


Figure 1: Phrase classification accuracy. Figure 2: Task-adaptive precision allocation.

replacing this with a small, lightweight learned classifier to enhance generalizability without significantly increasing computational overhead.

Building on this accurate phase detection, TSAR demonstrates a sophisticated, task-aware approach to resource management, as illustrated in Figure 2. The framework learns to dynamically allocate precision based on the complexity and nature of the dataset. For the highly complex AIME dataset, the highest precision is allocated to Problem Formulation (PF) (3.56 bits), emphasizing the need to correctly understand and set up the problem. In contrast, for the arithmetically-focused GSM8k dataset, the highest precision is shifted to Solution Verification (SV) (3.62 bits), reflecting the critical importance of rigorously checking the final computed answer. This adaptive behavior confirms that TSAR does not use a one-size-fits-all policy; instead, it intelligently distributes computational resources to the reasoning phases where they are most impactful, tailoring its strategy to the unique demands of each task.

E COMPLETION INDICATORS

To implement natural termination, we employ confidence-based completion phrase injection. The contextually appropriate completion indicators employed in our experiments are as follows,

- **Prompt 1: Final Answer** The usage of this prompt stems from our empirical observation of model outputs. We consistently observed that the model generates the token sequence `Final Answer` immediately preceding its final output. We therefore hypothesize that this prompt effectively triggers early exit behavior. Experimental results demonstrate that while this prompt achieves excellent truncation performance, it inadvertently suppresses the generation of the solution reasoning component, thereby exerting non-negligible negative impacts on final accuracy.
- **Prompt 2: Okay, I think I have finished thinking.** This formulation draws inspiration from Ma et al. (2025a), where the original work employed it at the beginning of model outputs to skip chain-of-thought reasoning. We posit that inserting this prompt within reasoning chains can effectively induce early exit. Our experiments reveal that this prompt maintains an optimal balance between truncation efficiency and solution reasoning length, consequently enabling the model to simultaneously optimize both token generation quantity and prediction accuracy.

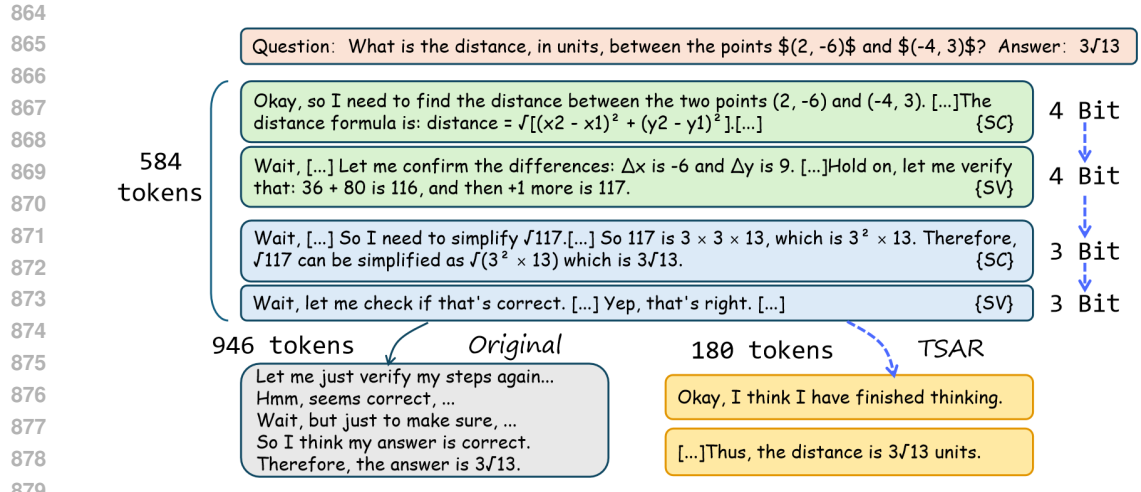


Figure 3: A case study demonstrating TSAR’s optimization process. TSAR identifies reasoning phases, adaptively reduces precision for computational steps, and terminates early upon reaching a stable conclusion, pruning the redundant verification steps.

F CASE STUDY

To provide a granular view of our framework’s mechanics, we present a case study on a challenging problem from the MATH-500 dataset. This analysis contrasts the lengthy, resource-intensive reasoning process of the original DeepSeek-R1-Distill-Qwen-7B model with the highly efficient, adaptive process guided by our TSAR framework. The comparison, illustrated in Figure 3, reveals how TSAR dynamically prunes both spatial and temporal redundancy without compromising the final answer’s accuracy.

It can be observed that after generating 584 tokens, the original model continues to produce an additional 946 tokens. In contrast, when applying our TSAR (Token-Scalable Adaptive Reasoning) method, the bit allocation process (indicated by blue arrows) can be observed, and the corresponding text output is nearly identical to that of the original model. Upon detecting that the reasoning quality meets the coordinated early-termination criterion, TSAR inserts the phrase "Okay, I think I have finished thinking." to halt further generation by the original model. Subsequently, the quantized model with TSAR generates only 180 tokens before concluding the reasoning process.

Although both approaches ultimately produce correct answers, our TSAR method achieves dual improvements in temporal efficiency (reducing inference time) and spatial efficiency (optimizing computational resource usage).

903
904
905
906
907
908
909
910
911
912
913
914
915
916
917